ORIGINAL PAPER

The Effect of Oxygen Adsorption for Vacancy-Induced d^0 Magnetism in HfO$_2$ (110) Surface

Hui Jia[1] · Wenhao Liang[1] · Min Zhou[1] · Ensi Cao[1] · Zhi Yang[1] · Wentao Hao[1] · Yongjia Zhang[1]

Abstract

Based on the density functional theory, we investigated the electronic structures and magnetic properties of the oxygen adsorption on the defective cubic HfO$_2$ (110) surface. The adsorption capacities of the perfect and defective surfaces follow in the sequence as: oxygen-deficient model > perfect surface > hafnium-deficient model. When the oxygen molecules adsorb on the nonmagnetic perfect HfO$_2$ surface, the system has a local magnetic moment and the antiferromagnetic coupling is more stable. For the defective cubic HfO$_2$ (110) surface, it is found that the oxygen vacancy is more easy to form than the hafnium vacancy by comparing the vacancy formation energy. And the hafnium vacancy could induce a large magnetic moment while the oxygen vacancy alone could not. After adsorption of the oxygen molecule, the nonmagnetic oxygen-deficient HfO$_2$ model is transformed into the magnetic surface. On the contrary, the introduction of adsorbed oxygen molecule causes the magnetic moment of hafnium-deficient HfO$_2$ surface to reduce. Additionally, if the oxygen molecules adsorb on the defective HfO$_2$ (110) surface, the ferromagnetic coupling is energetically favorable.

1 Introduction

Dilute magnetic semiconductors (DMSs) doped with transition metals (TM) have attracted much attention over the last decades due to their possibility of manipulating charge and spin degrees of freedom in a single substance [1–4]. However, no persuasive evidence can confirm that the observed ferromagnetic is intrinsic since the magnetic TM dopants usually separate to form the ferromagnetic clusters or secondary phases [5–7], which are undesirable for practical applications. Recently, Coey et al. found that the HfO$_2$ thin film without any magnetic elements can exhibit room-temperature ferromagnetism (RTFM), which is called "d magnetism" since this magnetism is not induced by the localized unpaired electrons in the d or f states of TM elements [8].

As a promising wide-band gap semiconducting material, HfO$_2$ has received much attention due to its potential technological applications, such as high dielectric constant, spintronics, and replacement of SiO$_2$ [9, 10]. Many works have investigated the origin of d magnetism in undoped HfO$_2$. In the experiments, oxygen vacancy has been proposed to play an important role in the magnetic origin which can be easily formed in sample preparation processes under different oxygen atmosphere [8, 11–13]. Coey et al. suggested that the observed RTFM in HfO$_2$ thin film is closely related to O vacancy instead of Hf vacancy [8]. Liu et al. presented the experimental evidence that the ferromagnetic behaviors can occur by intentionally inducing oxygen vacancies in undoped HfO$_2$ nanorods. It showed that the observed ferromagnetism probably resulted from oxygen vacancies generated in the annealing process [12]. Ran et al. fabricated the highly oxygen-deficient HfO$_2$ thin films by sputtering and found that the obtained ferromagnetic moments were influenced by the amount of oxygen vacancy, since filling up O vacancies could destroy the ferromagnetic ordering in the highly O-deficient sample [13].

However, some reports based on first-principle calculations indicated that Hf vacancies result in the local magnetic

✉ Yongjia Zhang
zhangyongjia@tyut.edu.cn

1   Key Laboratory of Advanced Transducers and Intelligent Control System, Ministry of Education, College of Physics and Optoelectronics, Taiyuan University of Technology, Taiyuan 030024, People's Republic of China

moments and ferromagnetic coupling in undoped HfO_2. Pammaraju et al. have studied the possibility of intrinsic defectdriven ferromagnetism in HfO_2 and found that Hf vacancy could cause a high-spin defect state and stable short-range ferromagnetic coupling [14]. Weng et al. calculated the magnetic properties of the hole-doped HfO_2 system and suggested that the possible ferromagnetism should be ascribed to the holes introduced by the Hf vacancy [15]. Beltran et al. investigated the magnetism of Hf-deficient cubic (100) and (111) surfaces and proposed that the formation of Hf vacancies causes the creation of holes in the O $2p$ valence band and the magnetic moments are located on O atoms surrounding Hf vacancies [16]. More recently, Wang et al. put forward a new mechanism of the complex defects of oxygen vacancy-induced (CDOV) ferromagnetism, in which the magnetic moment mainly results from the d orbitals of low valence state Hf ions adjacent to the CDOV and suggested that each kind of oxygen vacancy alone cannot induce the magnetism on the surfaces [17].

Obviously, there are some controversies about the origin of d ferromagnetism in undoped HfO_2. It is noticed that the above calculations mainly focused on the vacancyinduced magnetism, ignoring the interaction between the oxygen molecules in the air and the surface of material. However, it is hard to avoid the oxygen molecules during the sample preparation and mensuration, especially, the origin of ferromagnetism is experimental studied by vacuum annealing and tempering in the air. The method of vacuum annealing not only introduces the vacancies but also introduces the adsorption and desorption of oxygen on the surface. Therefore, it is necessary to investigate the effect of oxygen adsorption on vacancy-induced d magnetism in HfO_2 surface. For cubic HfO_2, it is known that the (110) surface is most stable [18]. In this paper, we systematically investigate the electronic structures and magnetic properties of oxygen adsorption on cubic HfO_2 (110) surface with various surface vacancies. And the mechanism of the magnetic coupling is further discussed.

2 Computational Methods

All simulations are carried out using planewave pseudopotential method as implemented in the Vienna ab initio simulation package (VASP) [19–21]. The exchangecorrelation functional is treated within the generalized gradient approximation (GGA) [22]. The electron-ion interaction is presented using the projector-augmented wave (PAW) method [23, 24]. The periodic boundary condition along the c axis was employed for the surface with a vacuum region (10 Å) between surfaces to make sure that there was no interaction between them. The energy cutoff of 520 eV was used for the plane-wave expansion of the electronic wave function. Brillouin-zone integrations are approximated by using the special k-point sampling of Monhkorst-Pack scheme. In the calculations of cubic HfO_2 (110) surface, a mesh size of $5 \times 2 \times 2$ is used for k-point sampling. To obtain the equilibrium structures, we allowed the lattice constants and all atoms in the surface unit cells to relax. Good convergence was obtained with these parameters. The total energy was converged to be 1.0×10^{-4} eV/atom in the optimized structure.

3 Results and Discussions

### 3.1 Cubic HfO_2 (110) Surface with Various Vacancies

The perfect cubic HfO_2 (110) surface can be modeled by cutting from the relaxed bulk structure, as shown in Fig. 1a. In order to study the stability of various vacancy defects on cubic HfO_2 (110) surface, we calculated their vacancy formation energies by the following formula [25]:

$$E_f = (E_{\text{tot}}^v - E_{\text{tot}}^0 + n_i \mu_i)/n_i \tag{1}$$

where E_{tot}^v and E_{tot}^0 are the total energies of the surface with and without vacancy, n_i is the number of atoms removed, and μ_i is the chemical potential of the corresponding atom. For cubic HfO_2 (110) surface, there are only two types of neutral vacancy defects on the surface, i.e., oxygen vacancy (V_O^0) and hafnium vacancy (V_{Hf}^0). The results show that the formation energy of V_{Hf}^0 vacancy is about 12.63 eV, and it is 7.14 eV for V_O^0 vacancy. By comparing the formation energies of these two neutral vacancies, it is found that the formation energy of oxygen vacancy is lower than that of hafnium vacancy. This implies that the V_O^0 is more stable than V_{Hf}^0 in the cubic HfO_2 (110) surface. Figure 1b presents the total density of states (DOS) of the perfect HfO_2 (110) surface and indicates no spin polarization emerges around the Fermi energy level. This implies that the perfect HfO_2 (110) surface is nonmagnetic. To further understand the origin of the magnetism induced by various vacancies in the surface, we plot the total DOSs and partial DOSs of HfO_2 (110) surface with various vacancies, as shown in Fig. 1c, d. When one V_O^0 is present in the surface, the spinup and spindown states of total DOS are symmetric (see Fig. 1c), suggesting that the V_O^0 cannot induce the magnetism in HfO_2 (110) surface.

For the HfO_2 (110) surface with a single V_{Hf}^0 vacancy, the total DOS show an obvious spin split around the Fermi level, as shown in Fig. 1d, indicating that the existence of local magnetic moments. The partial DOS demonstrates that the spin split is mainly from the spin polarization of O $2p$ electrons. As the presence of V_{Hf}^0 can lead to a loss of donor charge, four $2p$ holes on O atoms are formed, leading to

Fig. 1 **a** The structure of perfect HfO$_2$ (110) surface, ochre balls, and red balls represent Hf and O atoms, respectively. The spin-resolved total DOS and partial DOSs for **b** the perfect HfO$_2$ (110) surface, **c** the HfO$_2$ (110) surface with one O vacancy, and **d** the HfO$_2$ (110) surface with one Hf vacancy. The vertical dotted line indicates the Fermi level. **e** The spin-density map (SDM) of the HfO$_2$ (110) surface with one Hf vacancy. The yellow iso-surfaces represent the charge density of spin up. The iso-value is 0.02 e/Å^3
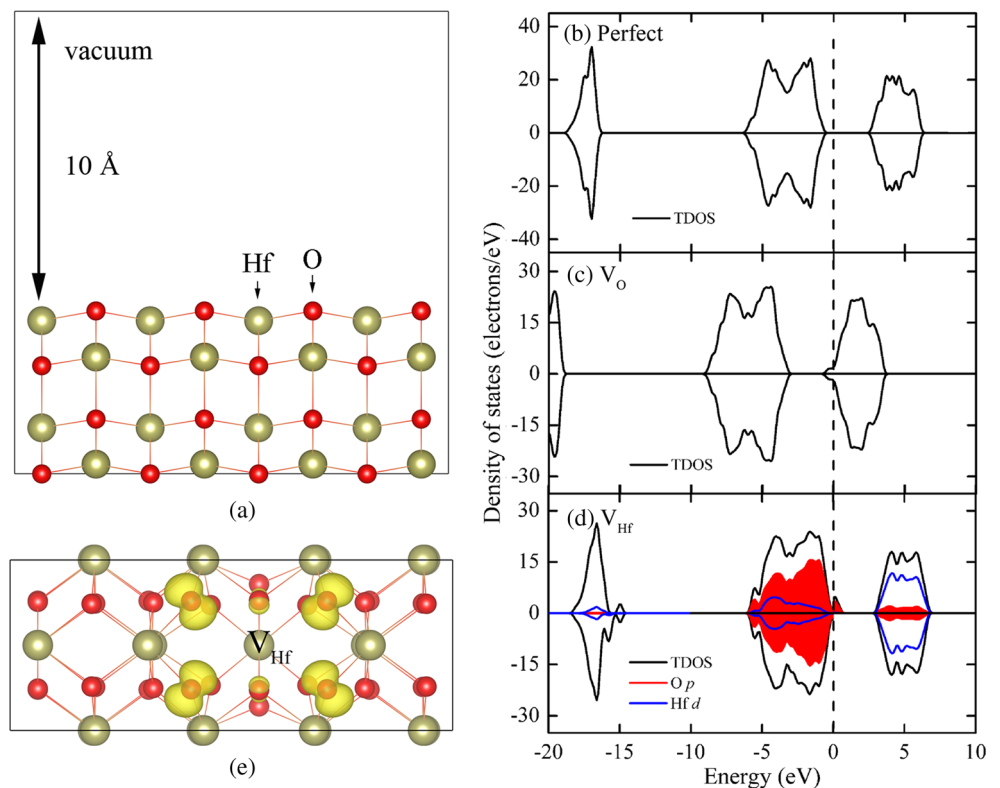
introduce the magnetic moments of about 4.0 μ_B. To further ascertain the origin of magnetism induced by V_{Hf}^0, we plot the three-dimensional spin-density distributions (spin up minus spin down) in Fig. 1e. The red balls and ochre balls represent the O and Hf atoms, respectively. When one V_{Hf}^0 exists in the HfO$_2$ (110) surface, the magnetization density is mainly distributed on the four 1st nearest-neighbor O atoms adjacent to the vacancy. In order to investigate the magnetic coupling characteristic between the local magnetic moments induced by V_{Hf}^0 vacancies, we consider the three distributions of two V_{Hf}^0 vacancies. These three distributions are the removal of two (a) 1st, (b) 2nd, and (c) 3rd nearest-neighbor Hf atoms from the surface, respectively. For each case, we calculate their relative energies between the ferromagnetic and antiferromagnetic couplings. The results show that the ferromagnetic coupling is energetically favorable in all cases, and the magnetic moments are 3.57, 3.97, and 3.44 μ_B, respectively. By comparing the total energies of these three cases, it is found that the system has the lowest energy when the double V_{Hf}^0 are located on the 3rd nearest neighbor, indicating that the V_{Hf}^0 vacancies could prefer to scatter in the surface. The above results are consistent with the earlier theoretical calculations [14, 15] but not very well explain the experimental results [8, 11–13]. Therefore, the effect of oxygen molecules chemisorbed on HfO$_2$ (110) surface is investigated further.

3.2 Oxygen Molecule Adsorbs on the Perfect HfO$_2$ (110) Surface

As a comparison, we first investigate the effect of adsorbed oxygen on the magnetism of perfect HfO$_2$ (110) surface. When oxygen molecule adsorbs on the perfect HfO$_2$ (110) surface, two initial orientations of the oxygen molecule are considered: one is vertical and the other is horizontal. For oxygen molecule adsorption on the perfect HfO$_2$ (110) surface, we calculated six initial configurations, as shown in Fig. 2, including P1 and P2 (O$_2$ molecule adsorption on the O atom of the surface), P3 and P4 (O$_2$ molecule adsorption on the Hf atom of the surface), and P5 and P6 (O$_2$ molecule adsorption on the hollow of the surface). For all cases, the initial distance between the oxygen molecule and surface is set to be 2.00 Å and the initial adsorption sites are marked with blue balls. The adsorption energy (E_{ads}) defined to be the difference between the energy of the O$_2$ molecule in the presence of the substrate and the sum of the separate energies of the adsorbed O$_2$ molecule with the substrate, which could be expressed as the following equation [26]:

$$E_{ads} = E_{substrate} + E_{adsorbate} - E_{substrate-adsorbate} \qquad (2)$$

where $E_{substrate+adsorbate}$ is the total energy of the substrate-adsorbate system in the stable state and $E_{substrate}$ and $E_{adsorbate}$ are the total energy of substrate and adsorbate,
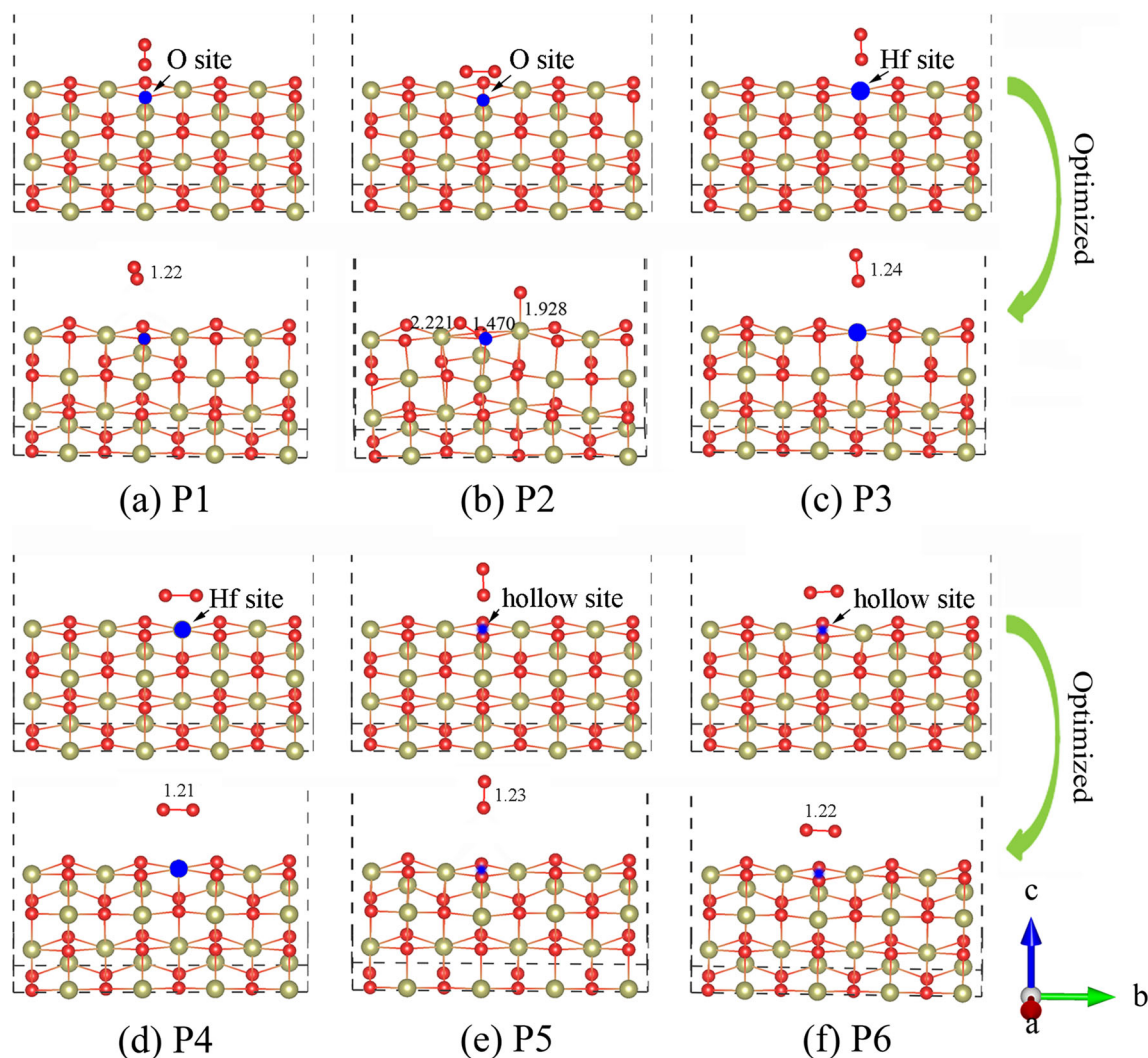
Fig. 2 The six adsorption configurations of the O_2 molecule adsorption on perfect HfO_2 (110) surface before and after optimization. The adsorption sites are marked with blue balls

respectively. In this definition, the positive E_{ads} indicates a stable adsorbed system, while the negative value corresponds to an unstable adsorbed system. Moreover, the electron-transfer between the oxygen molecule and the HfO_2 (110) surface is calculated by Bader charge analysis [27], which is defined as the electron difference between the adsorbed oxygen molecule and the isolated oxygen molecule [26, 28].

Figure 2 also displays the six adsorbed configurations after optimization. And the calculated results of the E_{ads}), the balanced distance (d) between the O_2 molecule and the surface, the O–O bond length of the O_2 molecule (d_{O-O}) and the charge transfer (q_{O_2}) are listed in Table 1. It can be seen that the balanced distances of P1, P3, P4, P5, and P6 configurations are 2.36, 2.34, 2.38, 2.47, and 2.45 Å, respectively. This indicates that the O_2 molecule in these five configurations is detached from the surface

after optimization, and the O_2 molecule cannot form any bond with the surface. For the P2 configuration, the bond of O_2 molecule is broken, as shown in Fig. 2b. One oxygen atom is combined with the surface oxygen atom, and the other is connected to the surface Hf atom. And the bond lengths of the newly formed bonds are 1.470 and 1.928 Å, respectively. The above results suggest that the O_2 molecule prefer to adsorb on the HfO_2 (110) surface with P2 configuration. Moreover, the value of E_{ads} for the P2 configuration is positive, indicating that this adsorption process is an exothermic reaction.

Because the O_2 molecule alone has a nonzero magnetic moment, the magnetic properties and density of states of the unabsorbed configurations are not considered. Figure 3a shows the total DOS and partial DOSs of the P2 configuration. A comparison between the total DOS of the perfect surface and that of the surface with one

Table 1 Calculated values of the adsorption energy (E_{ads}), the balanced distance (d) between the O_2 molecule and the surface, the O–O bond length of O_2 molecule (d_{O-O}) the Bader charges (q_{O_2})), and the magnetic moments (M_{tot}) for O_2 molecule adsorption on the perfect HfO_2 (110) surface

Configuration	E_{ads} (eV)	d(Å)	d_{O-O} (Å)	q_{O_2}(e)	M_{tot} (μ_B)
P1	–	2.36	1.22	0	–
P2	− 3.11	–	3.53	− 1.64	1.46
P3	–	2.34	1.24	0	–
P4	–	2.38	1.21	0	–
P5	–	2.47	1.23	0	–
P6	–	2.45	1.22	0	–

adsorbed O_2 molecule shows that the introduction of adsorbed O_2 produces an obviously spin-polarized impurity state around Fermi level. And this impurity state is mainly from the spin polarization of O 2p electrons, leading to the magnetic moment of 1.46 μ_B. Bader effective charge analyses demonstrate that the adsorbed O_2 molecule can obtain a total of 1.64 electrons from the surface, and these electrons will occupy the O 2p orbital. This confirms that the existence of the adsorbed O_2 molecule could lead to the rearrangement of electric charge in the surface. The three-dimensional spin-density distributions in the Fig. 3b show that the magnetization density is mainly distributed on the three O atoms adjacent to the adsorption site. To further investigate the magnetic coupling characteristic between the local magnetic moments induced by the adsorbed O_2 molecule, we compared the total energies of ferromagnetic and antiferromagnetic alignments of the perfect HfO_2 (110) surface with two adsorbed O_2 molecules. Two distributions of adsorbed O_2 molecules are considered: (a) the distance between two initial adsorption sites is 2.56 Å and (b) the distance between two initial adsorption sites is 3.44 Å. The calculated results indicate that the total energies of the state with antiferromagnetic coupling are found to be 76 and 53 meV lower than those of the state with ferromagnetic coupling. That is to say, the antiferromagnetic coupling is energetically favorable when O_2 molecules adsorb on the perfect HfO_2 (110) surface.

3.3 Oxygen Molecule Adsorbs on the Defective HfO$_2$ (110)

It is well known that the vacancies are easy to form during the material preparations. When oxygen molecule adsorbs on the oxygen-deficient HfO_2 (110) surface, eight configurations are designed, including M1 and M2 (O_2 vertically and horizontally adsorbs on the O atom around O vacancy), M3 and M4 (O_2 vertically and horizontally adsorbs on the Hf atom around O vacancy), M5 and M6 (O_2 vertically and horizontally adsorbs on the hollow around O vacancy), and M7 and M8 (O_2 vertically and horizontally adsorbs on the O vacancy). Similarly, the initial distance between the oxygen molecule and the HfO_2 (110) surface is 2.00 Å. These eight configurations before and after optimization are shown in Fig. 4, where the adsorption site is marked with blue balls. Obviously, the chemisorption between O_2 molecule and the surface occurs in each case. The corresponding E_{ads}), balanced distance (d), O–O bond length of O_2 (d_{O-O}), and charge transfer (q_{O_2}) are listed in Table 2. It is found that the d between the O_2 molecule and the surface for each configuration is smaller than 2.00 Å, and the O atom in the oxygen molecule forms the new chemical bond with the Hf atom around the vacancy. The bond length (d_{O-O}) of the O_2 molecule in each configuration becomes larger after optimization, suggesting that the O_2 molecule is activated. In addition,

Fig. 3 **a** Spin-resolved total DOS and partial DOSs for P2 configuration. The vertical dotted line indicates the Fermi level. **b** The SDM for P2 configuration. The yellow iso-surfaces represent the charge density of spin up. The iso-value is 0.01 e/Å^3
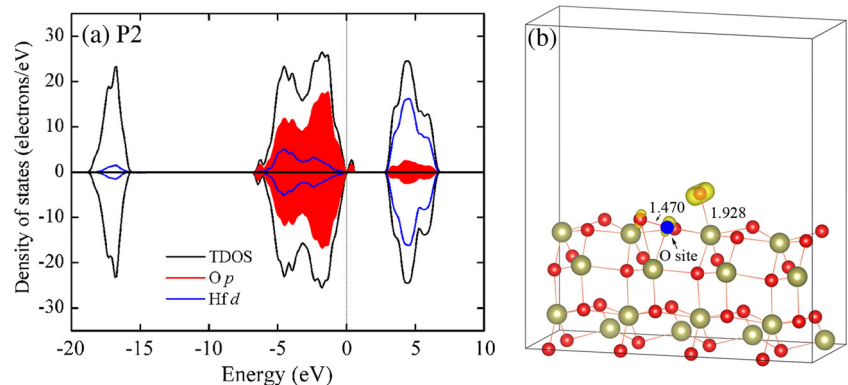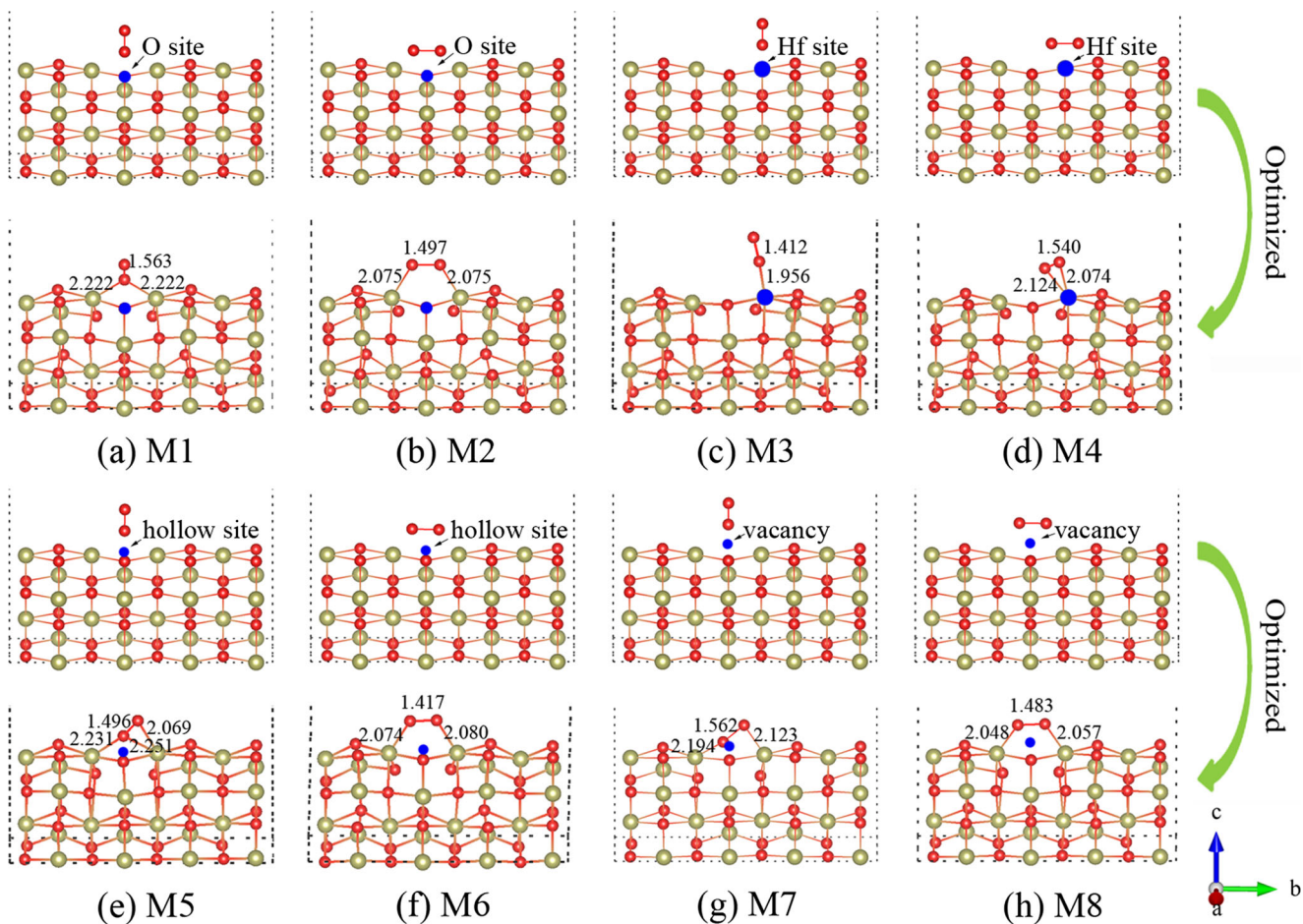
Fig. 4 The eight adsorption configurations of the O_2 molecule adsorption on HfO_2 (110) surface with O vacancy before and after optimization. The adsorption sites are marked with blue balls

the value of E_{ads} in each configuration is positive, and the M8 configuration has the largest adsorption energy. It shows that the O_2 molecule easily adsorbs on the above four adsorption sites, and the M8 is most stable in all optimized configurations. For the M8 configuration, the O_2 molecule horizontally adsorbs on the vacancy, and two O atoms in the molecule are respectively bridged with two Hf atoms surround the vacancy. From Table 2, it can be seen that the O_2 molecule acts as an acceptor in the adsorption process. With the exception of the M3 configuration, the number of the transferred electrons in other structures is about two electrons. For the M3 configuration, the oxygen molecule can obtain about one electron from the surface.

Figure 5 illustrates the total DOSs of all configurations and shows that no spin polarization emerges around the Fermi energy level for each configuration except M3 structure, indicating that these seven configurations are nonmagnetic. This is mainly due to the fact that the electron transfer after oxygen adsorption can lead to the rearrangement of the surface charge, and the unpaired

electrons are not generated during this process. In the M3 configuration, the oxygen molecule vertically adsorbs on the surface Hf atom, and one electron from Hf atom transfers to the oxygen molecule. This leads to the generation of an obvious spin split around the Fermi level in the total DOS of the M3 configuration, as shown in Fig. 5c, suggesting the existence of local magnetic moment. The partial DOS shows that the spin split is mainly from the spin polarization of O $2p$ electrons, and the system has a magnetic moment of -0.93 μ_B. In order to understand the nature of spin polarization for the M3 configuration, we plot the three-dimensional spin-density distributions in the inset of Fig. 5c. Clearly, the magnetization density is mainly distributed on the adsorbed O_2 molecule, and two oxygen atoms in the molecule share the electron obtained from the surface. To further deal with the effect of the magnetic coupling between two adsorbed O_2 molecule, two distributions of O_2 molecules in the oxygen-deficient HfO_2 (110) surface are investigated. Both oxygen molecules vertically adsorb on the Hf atoms around the vacancies, including (1) the distance between two initial adsorption

Table 2 Calculated values of the adsorption energy (E_{ads}), the balanced distance (d) between the O$_2$ molecule and the surface, the O–O bond length of O$_2$ molecule ($d_{O–O}$) the Bader charges (q_{O_2}) and the magnetic moments (M_{tot}) for O$_2$ molecule adsorption on the HfO$_2$ (110) surface with a single O vacancy

Configuration	E_{ads} (eV)	d(Å)	$d_{O–O}$ (Å)	Q_{O_2}(e)	M_{tot} (μ_B)
M1	9.06	1.83	1.56	− 1.79	0
M2	7.20	1.99	1.49	− 1.67	0
M3	7.90	1.96	1.41	− 1.09	− 0.33
M4	5.70	1.87	1.54	− 1.68	0
M5	7.14	1.97	1.49	− 1.79	0
M6	6.10	1.73	1.48	− 1.70	0
M7	7.04	1.61	1.56	− 1.92	0
M8	10.00	1.89	1.41	− 1.66	0

sites is 3.397 Å and (2) the distance between two initial adsorption sites is 6.931 Å. The calculated results show that the total energy of the state with ferromagnetic coupling is found to be 31 and 88 meV lower than that of the state with antiferromagnetic coupling, respectively, indicating that the ferromagnetic coupling is more favorable.

When the O$_2$ molecule adsorbs on the hafnium-deficient HfO$_2$ (110) surface, eight configurations are considered,

Fig. 5 Spin-resolved total DOS for all configurations of the O$_2$ molecule adsorption on HfO$_2$ (110) surface with O vacancy after optimization. The vertical dotted line indicates the Fermi level. **b** The partial DOS and SDM of M3 configuration. The blue iso-surfaces represent the charge density of spin down. The iso-value is 0.01 e/Å^3
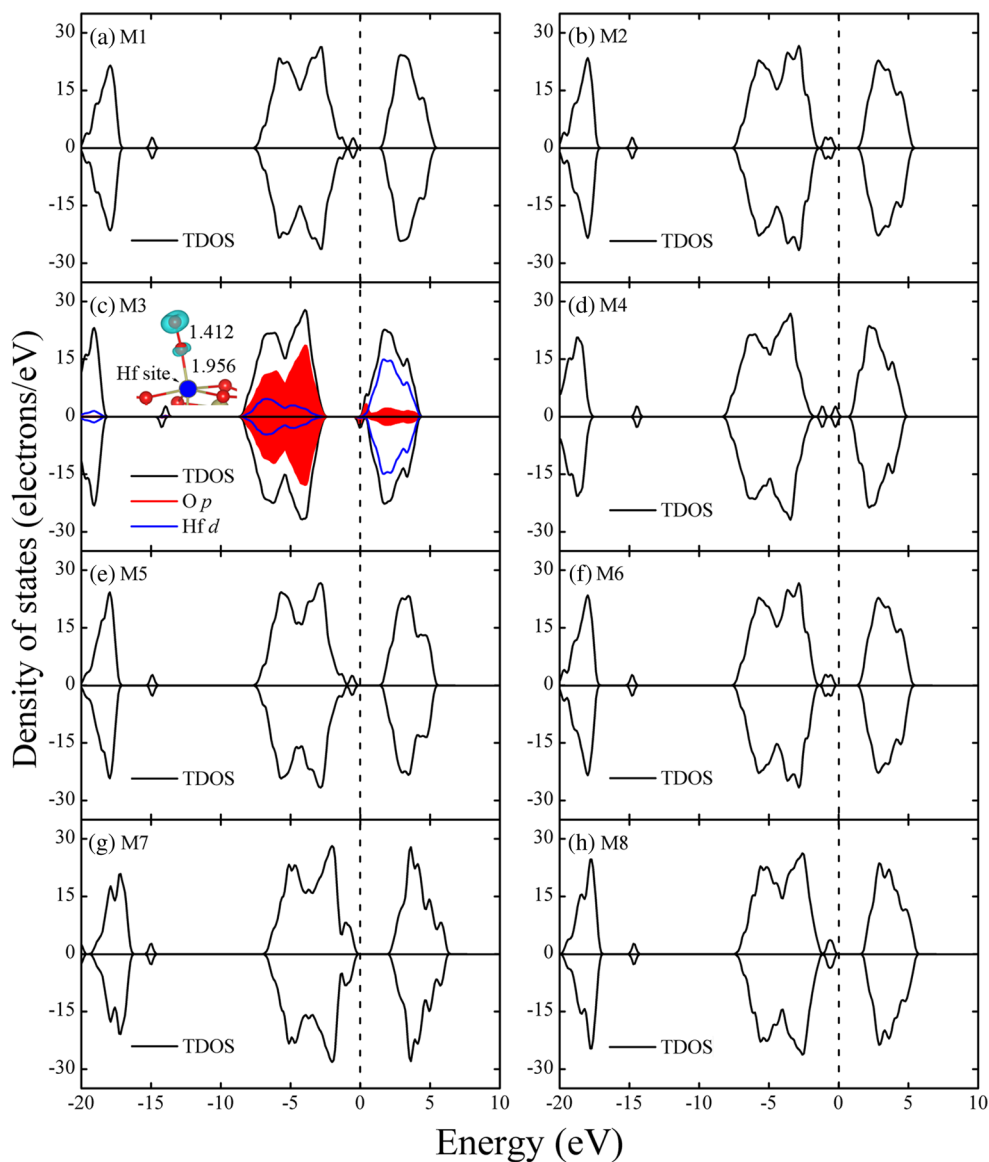
including L1 and L2 (the O_2 molecule vertically and horizontally adsorbs on the O atom around Hf vacancy), L3 and L4 (the O_2 molecule vertically and horizontally adsorbs on the Hf atom around Hf vacancy), L5 and L6 (the O_2 molecule vertically and horizontally adsorbs on the hollow around Hf vacancy), and L7 and L8 (the O_2 molecule vertically and horizontally adsorbs on the Hf vacancy). The corresponding optimized models of these configurations are shown in Fig. 6, and their E_{ads}, d, d_{O-O}, and q_{O_2} are all listed in Table 3. It can be seen that the distances between the O_2 molecule and the surface for the L1, L5, L6, L7, and L8 configurations are 2.74, 2.38, 2.41, 2.31, and 2.24 Å respectively, indicating that the O_2 molecule of these five configurations is detached from the surface after optimization due to the initial distances of 2.00 Å. For the other three configurations, the adsorbed O_2 molecule is close to the surface after optimization and some new chemical bonds are formed, as shown in Fig. 6b–d. The longer d_{O-O} of these three configurations shows that the adsorbed O_2 molecule is activated. The E_{ads} of these three

configurations are positive and that of L3 configuration are largest, indicating the adsorption of O_2 molecule with L3 configuration is most stable. Bader effective charge analyses show that the O_2 molecule is also an acceptor in these three adsorption processes, and it can obtain 0.43, 0.22, and 0.35 electrons from the surface, respectively.

Figure 7 shows the total DOSs, partial DOSs, and spin-density distributions of L2–L4 configurations. It is found that the spin up and spin down of the total DOS near the Fermi energy has an asymmetry and the magnetic moments mostly located on the adsorbed O_2 and the O atoms adjacent to the Hf vacancy. The existence of the rearrangement of the surface charge results in the magnetic moment of 2.94, 3.21, and 2.62 μ_B for these three configurations, respectively. For the hafnium-deficient HfO_2 (110) surface with two O_2 molecules, the magnetic coupling is also calculated. Because the L3 model is most stable in these three configurations, we consider two O_2 molecules vertically adsorbed on the surface Hf atoms around vacancies. And the distance between two initial adsorption sites is 7.188 Å.
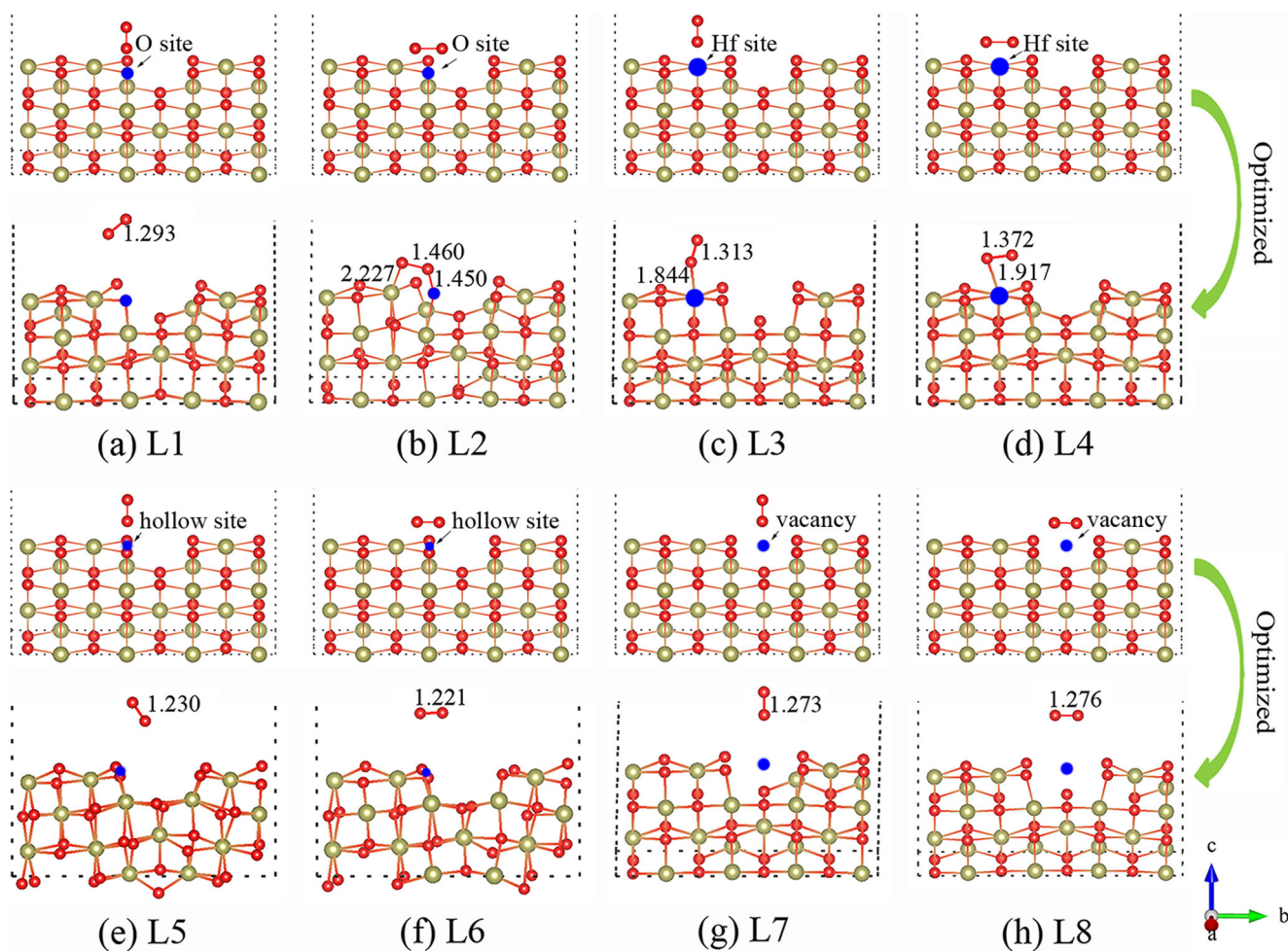

Fig. 6 The eight adsorption configurations of the O_2 molecule adsorption on HfO_2 (110) surface with Hf vacancy before and after optimization. The adsorption sites are marked with blue balls

Table 3 Calculated values of the adsorption energy (E_{ads}), the balanced distance (d) between the O_2 molecule and the surface, the O–O bond length of O_2 molecule (d_{O-O}) the Bader charges (q_{O_2}) and the magnetic moments (M_{tot}) for O_2 molecule adsorption on the HfO$_2$ (110) surface with a single Hf vacancy

Configuration	E_{ads} (eV)	d(Å)	d_{O-O} (Å)	Q_{O_2}(e)	M_{tot} (μ_B)
L1	–	2.74	1.29	0	–
L2	1.28	1.45	1.46	− 0.43	3.44
L3	2.12	1.84	1.31	− 0.22	3.21
L4	1.31	1.91	1.37	− 0.35	3.62
L5	–	2.38	1.23	0	–
L6	–	2.41	1.22	0	–
L7	–	2.31	1.27	0	–
L8	–	2.24	1.27	0	–

The results indicate that the energy of the ferromagnetic state is 73 meV lower than that of antiferromagnetic state, suggesting that the ferromagnetic coupling is more stable.

Up to now, many experimental and theoretical works have investigated the origin of d^0 magnetism in undoped HfO$_2$. In the experiments, the vacuum annealing enhances the RTFM, and the subsequent annealing in air reduces ferromagnetism, indicating that the observed ferromagnetism probably resulted from the oxygen vacancies generated in the annealing process [13]. Nevertheless, the existing theoretical calculations cannot explain this phenomenon well, and the calculated results suggest that the oxygen vacancies cannot induce any magnetic moment. Take into account the adsorption of oxygen molecule based on the existing theoretical analysis, there is a rational explanation for the above experimental results. The vacuum annealing leads to an increase in the number of oxygen vacancies on the surface of the material. After exposing the vacuum-annealed material in the air, the oxygen molecules would adsorb on the surface of material and the coexistence of oxygen vacancies and adsorbed oxygen molecules results in the enhancement of ferromagnetism (M3 configuration). In this process, fewer cation vacancies have less effect on the magnetic properties of the material, which can be ignored. The experimental results also show that the observed ferromagnetic signal is weakened after reannealing the material in the air [13]. This is mainly due to the fact that the oxygen vacancies are repaired in this reannealing process, and the number of oxygen vacancies on the surface is significantly reduced. On the other hand, when oxygen molecules adsorb on the hafnium-deficient model, the magnetic moment of the system also decreases (L2–L4 configurations). It should be noted that the oxygen molecules may also adsorb on the surface defect-free area in the whole experimental process. However, the antiferromagnetic state is more stable during this adsorption process (P2 configuration), which makes no contribution to the observed ferromagnetic signal.
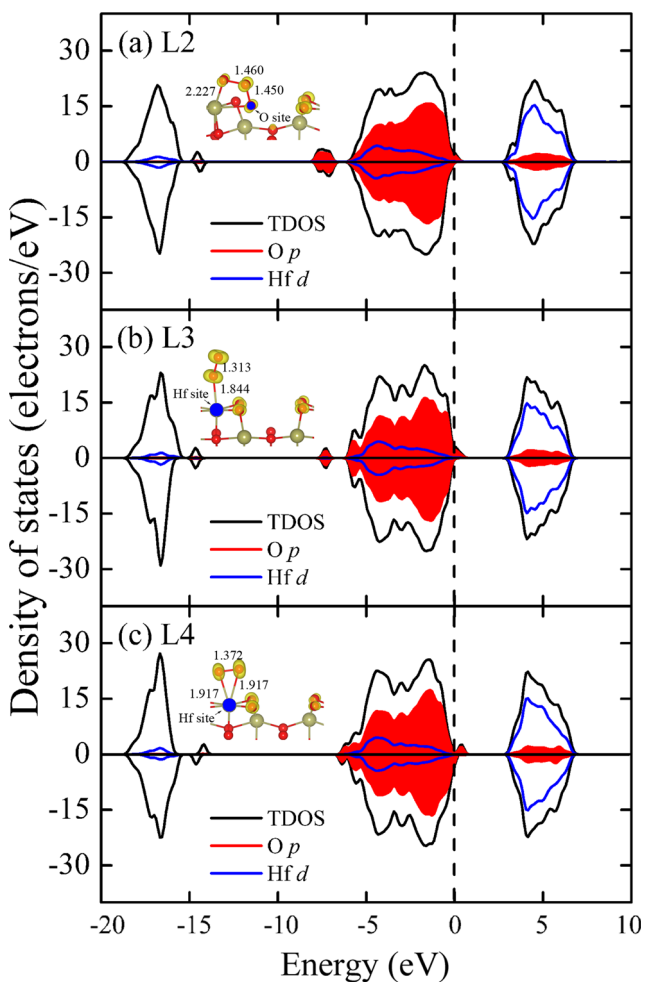

Fig. 7 Spin-resolved total DOSs, partial DOSs, and SDMs of **a** L2, **b** L3, and **c** L4 configurations. The vertical dotted line indicates the Fermi level. The yellow iso-surfaces represent the charge density of spin up. The iso-value is 0.01 e/Å^3

4 Conclusion

Based on the density functional theory, we investigated the electronic structures and magnetic properties of the oxygen adsorption on the defective cubic HfO$_2$ (110) surface. The adsorption capacities of the perfect and defective surfaces follow in the sequence as: oxygen deficient >perfect >hafnium deficient. By comparing the vacancy formation

energy, the oxygen vacancy is formed more easily than Hf vacancy, indicating that the number of oxygen vacancies is more than that of hafnium vacancies in HfO_2 (110) surface. For HfO_2 (110) surface, the oxygen vacancy alone cannot induce the magnetism. After adsorption of the oxygen molecule, the adsorbed O_2 molecule could induce the nonzero magnetic moment. On the contrary, the Hf vacancy alone could introduce a large magnetic moment, while the introduction of adsorbed O_2 molecule could decrease the magnetic moment in the whole system. Furthermore, when O_2 molecules adsorb on the perfect HfO_2 (110) surface, the antiferromagnetic state is more stable. For the other two adsorptive types, the ferromagnetic state is energetically favorable. The above calculation results can reasonably explain the existing experimental results: the vacuum annealing enhances the RTFM and the subsequent annealing in air reduces ferromagnetism.

References

1. Kitchen, D., Richardella, A., Tang, J.M., et al.: Atom-by-atom substitution of Mn in GaAs and visualization of their hole-mediated interactions. Nature **442**, 436–439 (2006)
2. Sato, K., Katayama-Yoshida, H.: Hyperfine interactions and magnetism of $3d$ transition-metal-impurities in II-VI and III-v compound-based diluted magnetic semiconductors. Hyperfine Interact. **136**, 737–742 (2001)
3. Deka, S., Joy, P.A.: Synthesis and magnetic properties of Mn doped ZnO nanowires. Solid State Commun. **142**, 190–194 (2007)
4. Wang, Y.Q., Yuan, S.L., Liu, L., et al.: Ferromagnetism in Fe-doped ZnO bulk samples. J. Magn. Magn. Mater. **320**, 1423–1426 (2008)
5. Park, J.H., Kim, M.G., Jang, H.M., et al.: Co-metal clustering as the origin of ferromagnetism in Co-doped ZnO thin films. Appl. Phys. Lett. **84**, 1338–1340 (2004)
6. Zhou, S., Potzger, K., Von Borany, J., et al.: Crystallographically oriented Co and Ni nanocrystals inside ZnO formed by ion implantation and postannealing. Phys. Rev. B **77**, 035209 (2008)
7. Kaspar, T.C., Droubay, T., Heald, S.M., et al.: Hidden ferromagnetic secondary phases in cobalt-doped ZnO epitaxial thin films. Phys. Rev. B **77**(R), 201303 (2008)
8. Venkatesan, M., Fitzgerald, C.B., Coey, J.M.D.: Thin films: unexpected magnetism in a dielectric oxide. Nature **430**, 630–630 (2004)
9. Demkov, A.A.: Investigating alternative gate dielectrics: a theoretical approach. Phys. Status Solidi B **226**, 57–67 (2001)
10. Zhao, X., Vanderbilt, D.: First-principles study of structural, vibrational, and lattice dielectric properties of hafnium oxide. Phys. Rev. B **65**, 233106 (2002)
11. Hong, N.H.: Magnetism due to defects/oxygen vacancies in HfO_2 thin films. Phys. Status Solidi (c) **4**, 1270–1275 (2007)
12. Liu, X., Chen, Y., Wang, L., Peng, D.L.: Transition from paramagnetism to ferromagnetism in HfO_2 nanorods. J. Appl. Phys. **113**, 076102 (2013)
13. Ran, J., Yan, Z.: Observation of ferromagnetism in highly oxygen-deficient HfO_2 films. J. Semicond. **30**, 102002 (2009)
14. Pemmaraju, C.D., Sanvito, S.: Ferromagnetism driven by intrinsic point defects in HfO_2. Phys. Rev. Lett. **94**, 217205 (2005)
15. Weng, H., Dong, J.: Ferromagnetism in HfO_2 induced by hole doping: first-principles calculations. Phys. Rev. B **73**, 132410 (2006)
16. Beltrán, J., Muñoz, M., Hafner, J.: Structural, electronic and magnetic properties of the surfaces of tetragonal and cubic HfO_2. New J. Phys. **10**, 063031 (2008)
17. Wang, M., Feng, M., Lu, Y.: Possible origin of ferromagnetism in undoped monoclinic HfO_2 film. Comput. Mater. Sci. **92**, 120–126 (2014)
18. Chen, G.H., Hou, Z.F., Gong, X.G.: Structural and electronic properties of cubic HfO_2 surfaces. Comp. Mater. Sci. **44**, 46–52 (2008)
19. Kresse, G., Hafner, J.: Ab initio molecular dynamics for open-shell transition metals. Phys. Rev. B **48**, 13115 (1993)
20. Kresse, G., Furthmüller, J.: Efficiency of ab-initio total energy calculations for metals and semiconductors using a plane-wave basis set. Comp. Mater. Sci. **6**, 15–50 (1996)
21. Kresse, G., Furthmüller, J.: Efficient iterative schemes for ab initio total-energy calculations using a plane-wave basis set. Phys. Rev. B **54**, 11169 (1996)
22. Perdew, J., Burke, K., Ernzerhof, M.: Generalized gradient approximation made simple. Phys. Rev. Lett. **77**, 3865–3868 (1996)
23. Blöchl, P.E.: Projector augmented-wave method. Phys. Rev. B **50**, 17953 (1994)
24. Kresse, G., Joubert, D.: From ultrasoft pseudopotentials to the projector augmented-wave method. Phys. Rev. B **59**, 1758 (1999)
25. Janotti, A., Van de Walle, C.G.: Native point defects in ZnO. Phys. Rev. B **76**, 165202 (2007)
26. Zhang, Y., Cao, E., Sun, L., et al.: Adsorption of NO on the $SrFeO_3$ (001) surface: a DFT study. Comp. Mater. Sci. **102**, 135–139 (2015)
27. Li, N., Sakidja, R., Ching, W.Y.: Ab initio study on the adsorption mechanism of oxygen on Cr_2AlC (0001) surface. Appl. Surf. Sci. **315**, 45–54 (2014)
28. Liu, X., Hu, J., Cheng, B., et al.: First-principles study of O_2 adsorption on the $LaFeO_3$ (010) surface. Sensor. Actuat. B-Chem. **139**, 520–526 (2009)